RESEARCH PAPER

Enhancement of Pseudomonas Aeruginosa Growth and Rhamnolipid Production Using Iron-Silica Nanoparticles in Low-Cost Medium

*Zahra Sahebnazar, Dariush Mowla * and Gholamreza Karimi*

Environmental Research Centre in Petroleum and Petrochemical Industries, School of Chemical and Petroleum Engineering, Shiraz University, Shiraz, Iran

ARTICLE INFO

Article History:
Received 14 October 2017
Accepted 25 December 2017
Published 01 January 2018

Keywords:
Addition time
Bacteria growth
Biosurfactant production
Nanoparticles concentration
Rhamnolipid

ABSTRACT

The application of iron-silica (Fe-Si) nanoparticles for the enhancement of the Pseudomonas aeruginosa growth and rhamnolipid production in molasses medium was studied. The experiments were designed based on the response surface method (RSM) to optimize growth and rhamnolipid production. The concentration of nanoparticles and the time required to add nanoparticles to culture medium were considered as independent variables. The dry weight of cell, the dry weight of rhamnolipid and the surface tension were measured as response variables. In addition, to determine a basic and low-cost medium, the concentrations of molasses and NaCl as components of medium were optimized by RSM. The optimum medium was estimated to include 15% of molasses without NaCl. The results showed that the highest increase in the growth of P. aeruginosa is 25% which occurred at 600 mg/L of nanoparticles and 18 h of addition time compared to the free-nanoparticles experiment. In the same way, the highest increase in rhamnolipid production was 57% at 1 mg/L of nanoparticles and 6 h of addition time compared to blank experiment. TEM images of the morphology changes of bacteria demonstrated the permeation of nanoparticles into the inbound cells. Results of this study reveal the great potential of Fe-Si nanoparticles to overcome the difficulties of the rhamnolipid production in industrial scale.

How to cite this article
Sahebnazar Z, Mowla D, Karimi G. Enhancement of Pseudomonas Aeruginosa Growth and Rhamnolipid Production Using Iron-Silica Nanoparticles in Low-Cost Medium. J Nanostruct, 2018; 8(1):1-10. DOI: 10.22052/JNS.2018.01.001

INTRODUCTION

Biosurfactants are amphiphilic molecules consist of hydrophobic and hydrophilic moieties produced by microorganisms (1). In recent years, an immense endeavor has been devoted towards biosurfactants owing to several advantages over chemical surfactants such as low toxicity, high biodegradability and ecological acceptability (2). The large-scale production of biosurfactants has been limited due to the low production yield (3). In order to solve these problems, various approaches were taken such as the use of cheap substrates (2), process optimization (4), and genetic engineering of organisms (5, 6). Recently, with the progress in nanotechnology science, the biosurfactant production has been approached to the use of nanoparticles (7, 8), because microorganism growth and biosurfactant production are conducted in nanometer scale. The presence of nanoparticles increases the rate of biochemical reactions due to their high specific surface areas (9, 10). Therefore, in the cellular level, the reaction of elements as nanoparticles is much faster than that those dissolved as ions (11, 12).

* *Corresponding Author Email: dmowla@gmail.com*

Among essential elements for biosurfactant production, Fe is the key metal for growth and biosurfactant production for several microorganisms such as actinobacteria (13) because some bacteria can employ Fe as either electron donors or acceptors in their energy metabolism (14) and the activator of the medium (7). On the other hand, silica nanoparticles are hydrophilic and have surface hydroxide groups that can be easily dispersed in water-based fluids such as culture medium used for growth of microorganism (15, 16). Therefore, in the composite of Fe-Si, the silica part of the nanoparticle can improve the dispersion and the stability of nanoparticles while the iron part can provide the needed Fe for bacteria.

Biosurfactant production by Pseudomonas aeruginosa has been extensively investigated (17). Pseudomonas species has been abundantly used for treating petroleum pollutions and enhancing oil recovery (18, 19) and can be considered as the best candidate for the production of biosurfactants (20). Despite the importance of rhamnolipid production, the effect of nanoparticles on rhamnolipid production by P. aeruginosa has not yet been studied.

Therefore, in this work, the combined effect of Fe-Si nanoparticles on the growth of P. aeruginosa and rhamnolipid production was investigated. The effects of both nanoparticles concentration and, for the first time, the addition time of nanoparticles to the culture medium were optimized by RSM. Also, to decrease the cost, molasses and NaCl were utilized as culture medium. Molasses and NaCl concentrations were also optimized by RSM and considered as the basic medium for experiments.

MATERIALS AND METHODS

Materials

All the chemicals (methanol, chloroform, HCl, NaCl) and biochemicals (nutrient broth, blood agar) used in this study were obtained from Merck Company. Molasses used as the culture medium for P. aeruginosa provided by a local sugar company in Marvdasht, Fars, Iran. The macro-elements of the molasses were determined by an elemental analyzer instrument (model: Eager 300 for EA1112) and the trace elements of molasses were measured by a spectrometer (optima 8000 ICP-OES model) (Table 1). P. aeruginosa was obtained from Microbial Collection of University of Tehran, Iran.

Table 1. The weigh percentage of components involved in molasses.

Component	Dry weight (%wt)
Carbon	31.001
Nitrogen	1.188
Hydrogen	6.550
Phosphor	0.014
Potassium	1.510
Sodium	1.260
Iron	0.006
Manganese	0.001
Zinc	0.001
Calcium	0.300
Copper	0.0003
Magnesium	0.035

Nanoparticles Synthesis

Zero-valent iron nanoparticles were synthesized as reported by Liu et al. (21). 8 g of $FeSO_4.7H_2O$ was dissolved in 400 mL of methanol/deoxygenated water solution (30% v/v), with pH of 6. 20 mL of $NaBH_4$ (2.1 M) was added dropwise to the mixture while stirring. After centrifugation at 8000 rpm for 20 min, the resultant sediment was washed several times with aqueous methanol solution (50% v/v) and kept in methanol solution under argon for later use. Nanostructured silica was synthesized as reported by Wang and Liu (22). 20 g of surfactant P123 was dissolved in HCl (2.0 M) and mixed with 37.5 g of TEOS at 40 °C for 20 h. Afterwards the mixture was heated for 24 h at 100 °C without agitation. Silica nanoparticles were filtered, washed and dried at room temperature for 12 h. Finally, to remove the surfactant, silica nanoparticles were heated at 540 °C for 5 h.

The immobilization of zero-valent iron nanoparticles on silica nanoparticles was performed as described by Saad et al. (23). 1 g silica nanoparticles was impregnated with $FeSO_4.7H_2O$ (1.2 M) and was suspended in 10 mL deionized water, then solution was mixed with 20 mL of $NaBH_4$ (2.4 M). The resultant black nanoparticles were centrifuged, washed three times with aqueous methanol solution (50% v/v) and dried at room temperature for 12 h. The final Fe-Si nanoparticles were kept at 4 °C for further use. Transmission electron micrographs (TEM) were recorded using a Philips CM30, (Netherlands). Energy dispersive X-ray spectroscopy analysis (EDAX, America) showed the elements of Fe-Si nanoparticles. X-ray diffraction (XRD) patterns were obtained using Cu Kα radiation (wavelength 1.5406) on a Siemens (D5000) diffractometer.

Determination of Optimum Medium for Bacteria Growth and Biosurfactant Production

To determine a basic and optimum medium for all experiments in this study, the concentration of molasses and NaCl as the components of culture medium were optimized by the RSM. The RSM was carried out with central composite design by Design Expert software (version 7.0). NaCl was added to molasses to investigate the tolerance of P. aeruginosa toward salinity for future application in petroleum industry. The percentage of molasses (1, 8 and 15 wt%), as well as the percentage of NaCl (0, 3 and 6 wt%) were selected for codes of -1, 0, +1 as shown in Table 2. Dry cell weight was chosen as the response. The suggested experiments were performed in 250 mL flasks containing 60 mL of culture medium inoculated with 1% (v/v) seed culture ($OD_{600\,nm}$ = 0.8–0.9). Culture mediums were prepared in different concentrations of molasses and NaCl according to Table 2. Molasses was diluted with tap water and pH was adjusted to 7.0. The cultures were incubated at 180 rpm at 38 ºC for 96 h. Samples were taken every 24 h to assess dry cell weight and emulsification index (E_{24}%). The surface activity of the produced biosurfactant in the optimum medium was evaluated by measuring surface tension and critical micelle concentration (CMC).

Determination of Optimum Conditions for Bacteria Growth and Biosurfactant Production Using Fe-Si Nanoparticles

The effect of nanoparticles on the growth of P. aeruginosa and rhamnolipid production was investigated and optimized using the RSM. The nanoparticles concentration and the addition time were considered as independent variables (Table 3). Different concentrations of nanoparticles (1, 600 and 1200 mg/L), as well as various addition time (6, 11 and 16 h) were selected for levels of -1, 0, +1, respectively. The dry weight of cell and the dry weight of biosurfactant were chosen as the responses. P. aeruginosa was cultured in the optimum medium included 15% molasses and 0% NaCl at 38 °C and 180 rpm for 96 h. Fe-Si nanoparticles were sterilized by ethanol, were suspended in deionized water and dispersed with ultrasonic bath (Parsonic, Iran) for 30 min at 38 °C. Fe-Si nanoparticles' suspensions were added to the mediums of bacteria at various times of bacterial growth according to designed experiments by the RSM. Sampling was conducted every 24 h for the

Table 2. Experimental design for the optimization of medium by RSM.

Culture medium	NaCl Concentration (% wt)	Molasses Concentration (%wt)
1	0	1
2	6	1
3	0	15
4	6	15
5	0	8
6	7.2	8
7	3	1
8	3	17.9
9	3	8
10	3	8
11	3	8
12	3	8
13	3	8

Table 3. Experimental design for the optimization of biosurfactant production using Fe-Si nanoparticles by RSM.

Run Number	Nanoparticles Concentration (mg/L)	Addition time (h)
1	1	6
2	1	16
3	1200	6
4	1200	16
5	600	4
6	600	18
7	0	11
8	1446	11
9	600	11
10	600	11
11	600	11
12	600	11
13	600	11

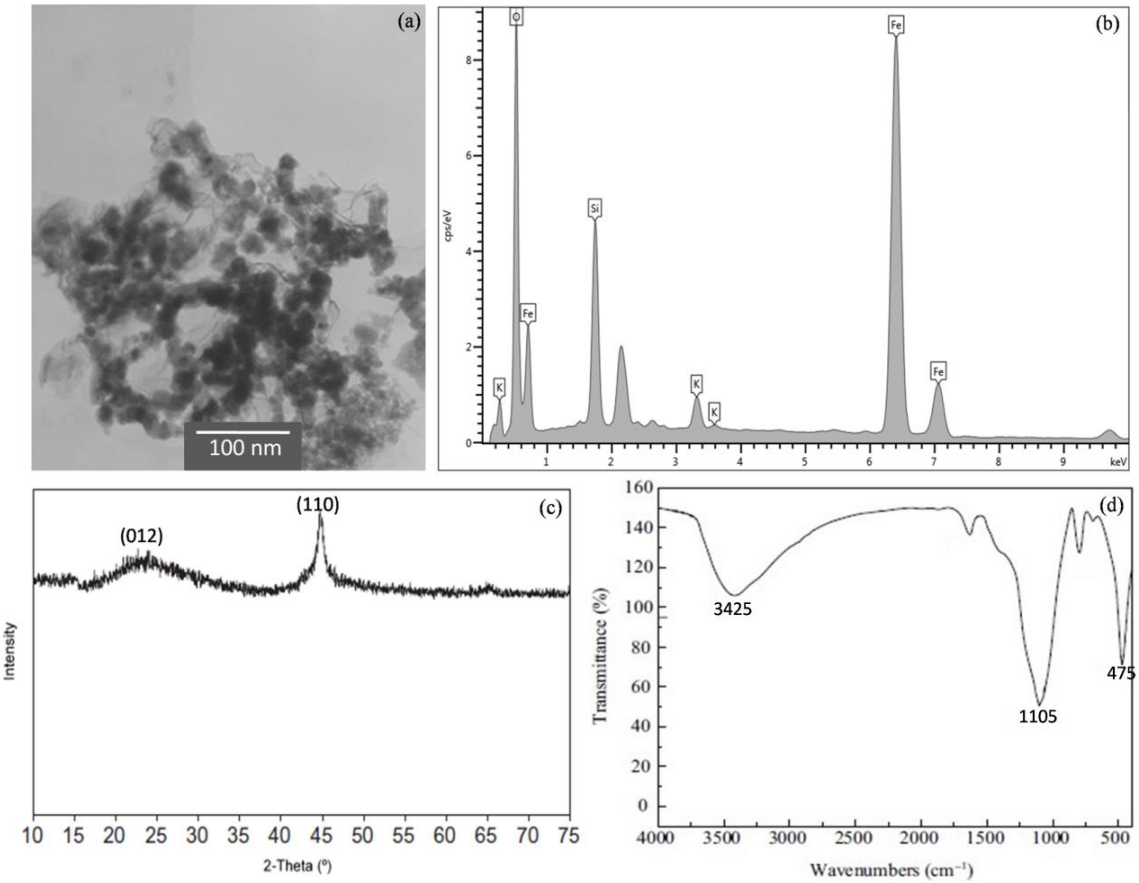

Fig. 1. Characterization of Fe-Si nanoparticles a) TEM image at 100 nm; b) EDX result; c) XRD spectra; d) FT-IR spectra.

measurement of dry weight of cell, dry weight of rhamnolipid and surface tension. The morphology of the bacteria and its interaction with the Fe-Si nanoparticles were obtained using TEM (PHILIPS CM30, Netherlands) after 14 h of bacteria-nanoparticle inoculation. For this purpose, 1 mL of culture was centrifuged at 1000 ×g for 10 min and the settled cells were suspended in phosphate-buffered saline (PBS). The suspension was added to a 400 mesh Cu grids overlaid with a thick carbon films and then TEM images were taken.

Analytical Methods

To measure the dry cell weight, 5 mL aliquot of the fermentation broth was centrifuged at 11,000 ×g for 25 min at 4 °C. The cell pellet was dried in oven to a constant weight. The cell free supernatant was used to extract and measure the produced biosurfactant. Extraction was performed by acid precipitation of supernatant to pH about 2.0 and the resultant sediment was washed by solvents of methanol and chloroform with a volume ratio of 1:2. The washed sediment was dried in a rotary vacuum evaporator and weighted (24). E_{24}% was measured as described by Cooper and Goldenberg (25). The surface tension of cell free supernatant was measured with a digital tensiometer (KSV, Finland, Sigma 703) using Du Nouy ring method. CMC of samples of biosurfactant solution were measured as reported by Diniz Rufino et al (26).

Stability of Biosurfactant

To study the stability of produced biosurfactant in extreme conditions, the cell free broth was incubated at 50, 75 and 90 °C for 12 days and cooled to room temperature after which the surface tension was measured. The pH stability of the cell free broth was investigated by changing the pH from 8.5 to 3 using HCl solution (6 N) and then measuring the surface tension after 45 days. In order to assess the effect of salinity on the surface activity of the cell free broth, various NaCl concentrations (10–25%, w/v) were employed for 45 days.

RESULTS AND DISCUSSION

Characterization of Fe-Si nanoparticles

The results of TEM showed that nanoparticles have a spherical shape (Fig. 1a). The Fe-Si nanoparticles were about 30 nm in diameter. Energy dispersive X-ray spectroscopy analysis showed that elements of Fe, Si and O exist in nanoparticle (Fig. 1b). The weight percentage of silica and iron of the Fe-Si nanoparticles is 13.17% and 56.85%, respectively. XRD analysis of the Fe-Si nanoparticles (Fig. 1c) demonstrated the presence of zero-valent iron and silica at 2θ = 45 and 22, respectively. The existence of iron and silica can also be demonstrated by FT-IR spectra (Fig. 1d). A broad band centered at 3425 cm^{-1} due to the adsorbed water and hydroxyl groups is observed. Also the strong band centered at 1105 cm^{-1} is related to the Si–O–Si structure (27). The absorption peak at 475 cm^{-1} is attributed to the Fe–O structure (28).

Optimization of Cultivation Medium Using Molasses and NaCl

Results of bacterial growth using different concentrations of molasses and NaCl at 24 h were illustrated in Fig. 2a. Based on these data, optimization of bacterial growth was performed by design expert software. R^2 value of 0.96 shows that the model can predict the response reasonably in good agreement. The model was found to be significant with $p < 0.005$ as shown in Equation (1):

$$R1=12.61 - 3.01A + 2.11B - 2.62AB - 5.23A^2 - 2.73B^2$$

Where R1 is dry cell weight, A is NaCl concentration, and B is molasses concentration. The maximum bacteria growth is observed in nearly maximum molasses concentration and nearly minimum NaCl concentration (Fig. 2b). Fig. 2a shows that the most growth was occurred in 15% of molasses because molasses is rich in sucrose and glucose as carbon source. Joshi et al. (2) observed similar results. Although bacterial growth and biosurfactant production using molasses as the sole carbon source has been studied by Al-Bahry et al. (29) and Dubey et al. (30), but `they added other compounds as nitrogen source and trace elements in addition to molasses. The dilution of molasses with tap water, without addition of trace elements and nitrogen source, pointed that the process applied in this study could be cost-effective when applied at industrial scale. As shown in Fig. 2a, when NaCl concentration increased from 0 to 3%, bacteria continued to grow and tolerate the salinity up to 3%. This result is in accordance with data obtained by Kiran and Lawrance (31, 32). They demonstrated the maximum NaCl concentration for the bacteria growth and the biosurfactant production was 3%. According to Fig. 3, a stable emulsion for more than 45 days can be produced in the absence of NaCl and at high concentrations of mlasses. Emulsification index represents the ability of biosurfactant production by P. aeruginosa. As shown in Table 1, molasses has low nitrogen

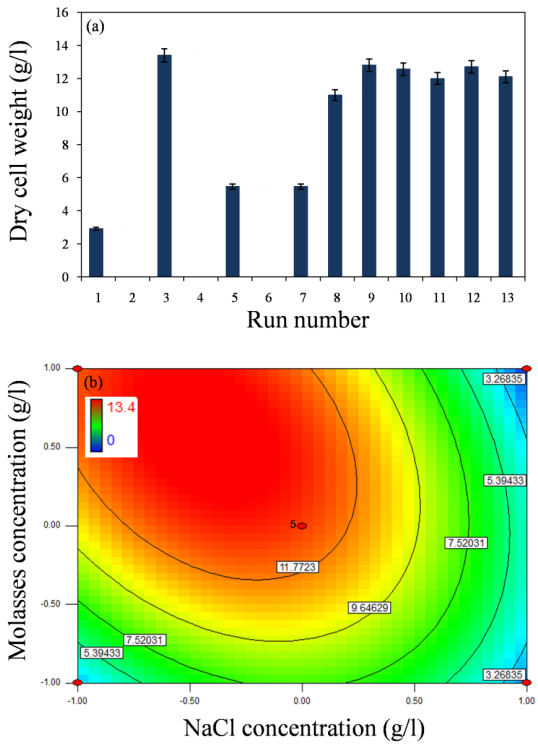

Fig. 2. Optimization of dry cell weight based on different concentrations of molasses and NaCl after 24 h of fermenttion a) at various runs; b) as contour plots.

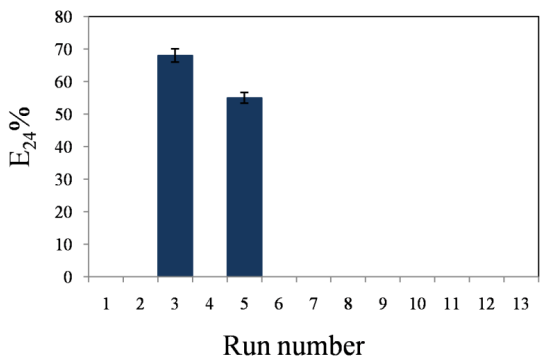

Fig. 3. Variation of E24% for various runs with different concentration of NaCl and molasses.

concentration and high C/N ratio of approximately 31. Biosurfactant production can be attributed to high expression of porin OprE involved in transmembrane transport. The porin OprE is a rhlAB expression activator at nitrogen-limiting conditions. Rhamnolipid production is catalyzed by two enzymes of RhlA and RhlB encoded by rhlA and rhlB genes, therefore rhamnolipid is produced significantly in molasses with high C/N ratio (33).

The NaCl free medium (0% NaCl) containing 15 wt% of molasses was chosen as the basic medium based upon the results of optimum concentration and emulsion index. Therefore, all subsequent experiments were performed with this medium in the presence of nanoparticles.

Surface Activities of Produced Biosurfactant at Optimum Medium

The surface tension of cell free broth reduced from 48.46 mN/m at culture medium without bacteria to 30.80 mN/m at optimum medium with bacteria. CMC of the produced biosurfactant was found to be 350 mg/L (Data not shown). The CMC of the biosurfactants produced by P. aeruginosa in present study are in accordance with the previously reported values (34). Briefly, the produced biosurfactant by P. aeruginosa displayed excellent surface activity at optimum medium.

Interaction of Fe-Si Nanoparticles with P. aeruginosa

Effect of Nanoparticles on P. aeruginosa Growth

The effect of nanoparticles on the bacterial growth can be seen by measuring the dry weight of cell after co-incubation with nanoparticles. The results of the bacterial growth for the first day for all runs were plotted in Fig. 4a. Based on these results, the statistical optimization of bacterial growth was carried out by design expert software. The model was found to be significant with $p < 0.005$, $R^2 = 0.92$ and is given in Equation (2):

$$R2 = 14.32 + 0.8A - 0.97B + 0.75AB + 0.0056A^2 - 1.76B^2$$

Where R2 is dry cell weight, A is addition time, and B is nanoparticles concentration. The proposed model shows that the bacterial growth is significantly influenced by the nanoparticles concentration and addition time interactively. As seen in Fig. 4b, the maximum bacteria growth is observed for central value of nanoparticles concentration and maximum addition time.

As shown in Fig. 4a, low concentrations of nanoparticles did not change the growth, that it could be attributed to low concentrations of nanoparticles, which is not sufficient to affect on the bacteria growth. At concentration of 600 mg/L, Fe-Si nanoparticles not only did not show toxicity to the bacteria, but also increased the growth. The most bacterial growth related to the concentration of 600 mg/L increased by 25% compared to the control run. This increase could be due to the enrichment of the medium nutrition by Fe-Si nanoparticles which activate the bacteria (7). Furthermore, because of small size and high surface associated with nanoparticles, both permeation through the cell membrane and the microbiological reaction rates will be enhanced (12, 35). Also, the presence of Fe element provides the necessary electron and energy for bacteria, consequently, leads to bacterial growth (14, 36). Different results at runs with the same nanoparticles concentrations (for instance 600 mg/L) show that the addition time of nanoparticles to cultivation medium plays a significant role in the bacteria growth. Higher concentration of Fe-Si nanoparticles in cultivation medium resulted in decrement of bacterial growth. The decrease in the bacterial growth could be attributed to the cell membrane breakage. The damage of cell membrane of various bacteria by different nanoparticles, especially at high concentrations, has been reported in previous studies (8, 37, 38). Furthermore, higher concentrations of iron in the culture medium increase reactive oxygen species (ROS) which leads to the cell death (39, 40).

In almost all previous similar studies (7, 37, 41, 42), the results show that there is a critical concentration of nanoparticles which is detrimental for microorganisms. The critical concentration of Fe-Si nanoparticle in the present study was observed to be between 600 mg/L and 1200 mg/L. Further experiments should be carried out to determine the precise amount of critical concentrations of Fe-Si nanoparticles for P. aeruginosa. It is worth mentioning that the addition time has significant role in the determination of critical concentration as confirmed by Chaithawiwat et al. (43). Fig. 5 shows the TEM images of bacteria after 14 h of co-incubation with Fe-Si nanoparticles. Fig. 5a indicates that the cell membrane was damaged by Fe-Si nanoparticles which resulted in cell destruction. Additionally, Fig. 5b demonstrates the permeation of nanoparticles into the inbound cells

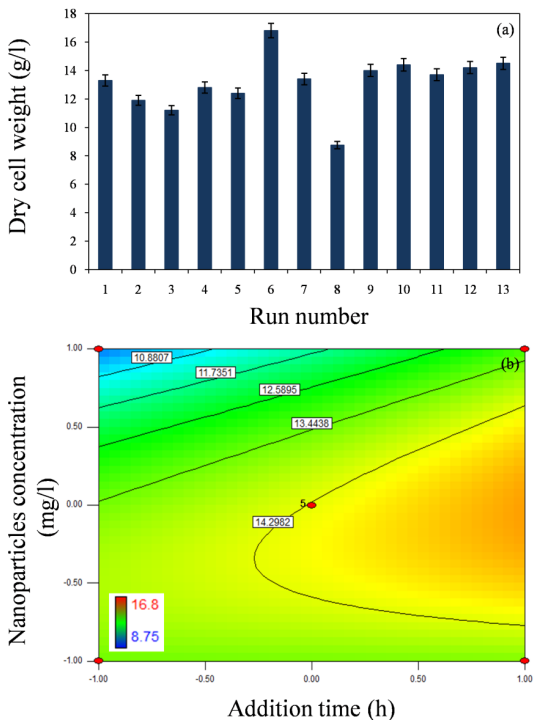

Fig. 4. Optimization of dry cell weight based on different nanoparticles concentration and addition time after 24 h of fermenttion a) at various runs; b) as contour plots.

which supplies necessary iron for the cell growth. These results were similar to the results of previous studies (44, 45).

Effect of Nanoparticles on Biosurfactant Production

The amount of produced rhamnolipid at 4th day for suggested runs by RSM is shown in Fig. 6a. Based on these data, statistical analysis of biosurfactant production was carried out by design expert software. The model was found to be significant with $p < 0.005$, $R^2 = 0.91$ and is given in the form of Equation (3):

$$R3= 9.68- 0.50A + 0.78B + 1.48AB$$

Where R3 is the dry weight of biosurfactant, A is addition time, and B is nanoparticles concentration. As depicted in Eq.3 and Fig. 6b, maximum biosurfactant production is obtained for two completely different situations namely: 1) where nanoparticles concentration and addition time are both minimum, 2) where nanoparticles concentration and addition time are both maximum. As demonstrated in Fig. 6a, more biosurfactant was produced for almost all concentration of nanoparticles, while bacterial growth decreased at higher concentrations of nanoparticles. The most increase in biosurfactant production was occurred at the concentration of 1 mg/L by 57% compared to the nanoparticle-free run.

The increase in biosurfactant production in all of concentrations of nanoparticles can be attributed to the presence of iron component. Previous studies concluded that iron element is a significant component for biosurfactant production by microorganisms (13, 14). Hassan et al. (20) reported that iron ion has the highest importance in rhamnolipid production by P. aeruginosa M2H2 14. Dehner et al. considered the bioprocess of iron assimilation by P. aeruginosa and concluded that three mechanisms can be involved: the formation

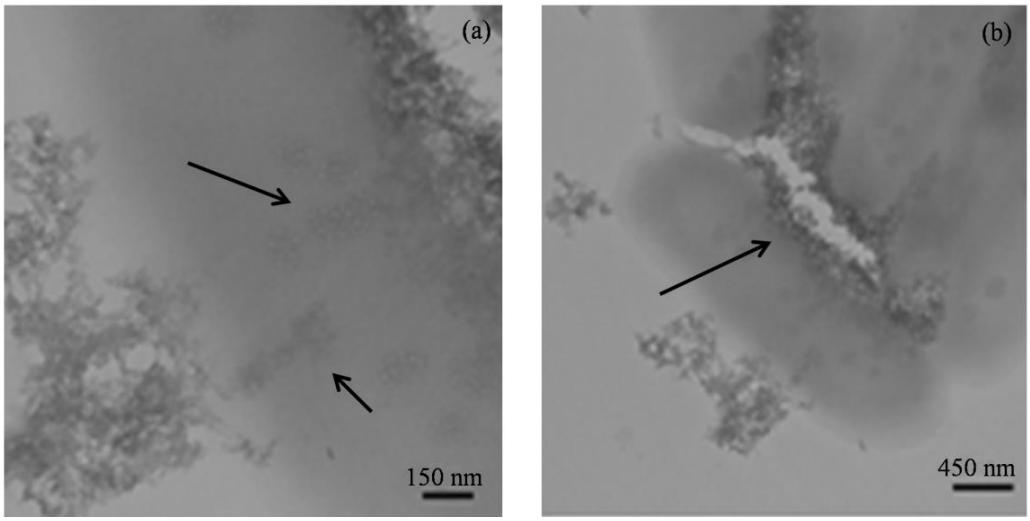

Fig. 5. TEM images of bacteria and Fe-Si nanoparticle interaction a) cell membrane destruction; b) permeation of Fe-Si nanoparticle into the cells.

of siderphore, the secretion of proteases, and the secretion of reductants such as blue-green pyocyanin to reduce Fe(III) to Fe(II) for more solubility and consequently more assimilation (46). In the present study, the color change of medium to blue-green demonstrated the secretion of pyocyanin for iron assimilation. Also they demonstrated that Fe(III)-pyochelin outer membrane receptor, protein related to iron assimilation, was more expressed in medium with high C/N ratio similar to medium used in this study. It is worth mentioning that the rate of biochemical reactions involved in the process of biosurfactant production using iron nanoparticles is much faster when iron ions are dissolved in the medium. This is due to high available active surface of nanoparticles (11).

At higher concentration of nanoparticles where the growth decreased, in addition to the previous mentioned reasons, the increase in biosurfactant production can be attributed to the secretion of produced biosurfactant from cell. In fact, biosurfactant is one extracellular metabolite and is liberated to exterior medium after it is produced (47, 48). The breakage of cell membrane at high nanoparticles concentrations facilitates the secretion of rhamnolipid to out of the cell.

The data of surface tension at 4th day of fermentation did not show significant difference for different runs. The amounts of surface tension in all runs were approximately equal and about 31-33 mN/m which explains that the concentration of biosurfactant has reached to its CMC.

Stability Studies

The data of stability test are shown in Figs. 7a to 7c, respectively. As shown in Fig. 7a, the surface tension of biosurfactant solution remained nearly constant at minimum value up to 90 °C for 8 days. For longer duration, the surface tension remained unchanged up to 75 °C. Furthermore,

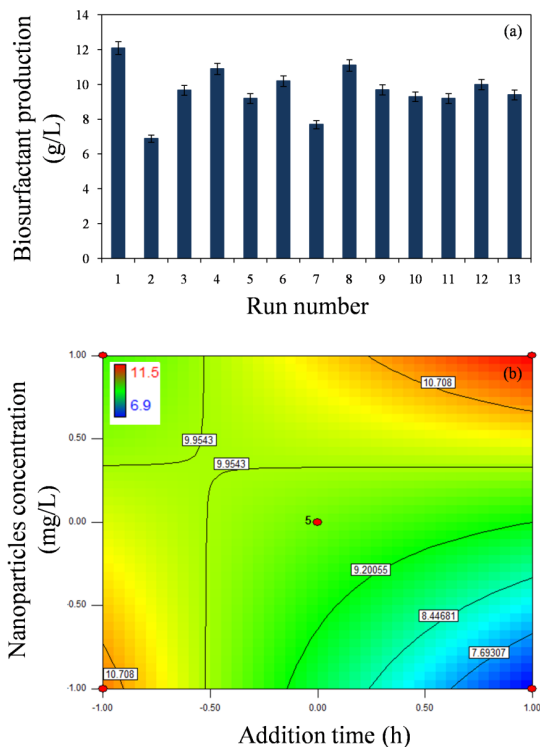

Fig. 6. Optimization of the dry weight of biosurfactant based on different nanoparticles concentration and addition time after 96 h of fermentation a) at various runs; b) as contour plots.

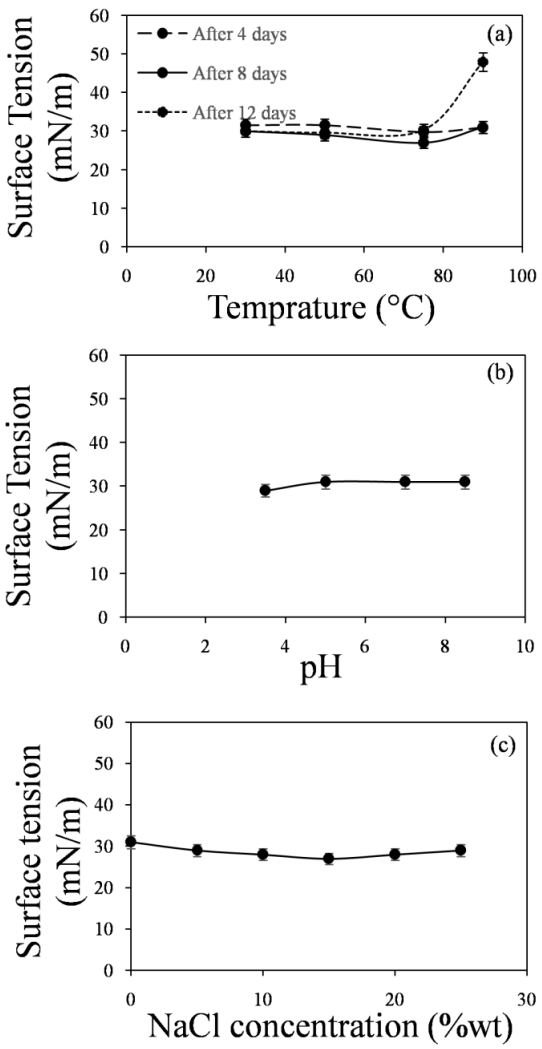

Fig. 7. Variation of surface tension with a) temperature; b) pH after 45 days; c) salinity after 45 days.

the produced biosurfactant was stable in the wide range of pH (Fig. 7b) and salinity (Fig. 7c) and the surface tension remained constant for 45 days. Although numerous studies have been done on biosurfactant stability for short duration (49-51), the present study demonstrates this parameter for long duration. The good stability of biosurfactant produced at long duration, gives a great potential for its utilization in petroleum industy.

CONCLUSION

In this study, Fe-Si nanoparticles were used to enhance the biosurfactant production by P. aeruginosa. The results of the experiments done based on RSM, showed that nanoparticles concentration and addition time of nanoparticles to culture medium were effective parameters on the enhancement of growth and rhamnolipid production. The maximum biosurfactant production was obtained at 1 mg/L concentration of nanoparticles and 6 h addition time. TEM images of bacteria and Fe-Si nanoparticles interaction illustrate the permeation of nanoparticles into the inbound cells and the supply of necessary iron for the biosurfactant production. The produced biosurfactant in the presence of nanoparticles revealed a significant stability at extreme conditions of temperature, pH and salinity for a long duration. To reduce the cost and consequently to increase the efficiency of biosurfactant production, especially in industry scale, the concentration of molasses and NaCl were optimized as culture medium. The optimum medium was considered to include 15% of molasses without NaCl. At the obtained optimum medium, biosurfactant showed a great surface activity. It is expected that the proposed procedure in this study can improve considerably the efficiency of biosurfactant production in industrial scale.

ACKNOWLEDGMENTS

The authors thank the National Iranian South Oil Company for the partial support to carry out this research.

CONFLICT OF INTEREST

The authors declare that there are no conflicts of interest regarding the publication of this manuscript.

REFERENCES

1. Satpute SK, Banpurkar AG, Dhakephalkar PK, Banat IM, Chopade BA. Methods for investigating biosurfactants and bioemulsifiers: a review. Crit. Rev. Biotechnol. 2010;30(2):127-44.
2. Joshi S, Bharucha C, Jha S, Yadav S, Nerurkar A, Desai AJ. Biosurfactant production using molasses and whey under thermophilic conditions. Bioresour. Technol. 2008;99(1):195-9.
3. Behary N, Perwuelz A, Campagne C, Lecouturier D, Dhulster P, Mamede A. Adsorption of surfactin produced from Bacillus subtilis using nonwoven PET (polyethylene terephthalate) fibrous membranes functionalized with chitosan. Colloids Surf., B. 2012;90:137-43.
4. Mouafi FE, Elsoud MMA, Moharam ME. Optimization of biosurfactant production by Bacillus brevis using response surface methodology. Biotechnol. Rep. 2016;9:31-7.
5. Youssef NH, Wofford N, McInerney MJ. Importance of the long-chain fatty acid beta-hydroxylating cytochrome P450 enzyme YbdT for lipopeptide biosynthesis in Bacillus subtilis strain OKB105. Int. J. Mol. Sci. 2011;12(3):1767-86.
6. Kryachko Y, Nathoo S, Lai P, Voordouw J, Prenner EJ, Voordouw G. Prospects for using native and recombinant rhamnolipid producers for microbially enhanced oil recovery. Int. Biodeterior. Biodegrad. 2013;81:133-40.
7. Liu J, Vipulanandan C, Cooper TF, Vipulanandan G. Effects of Fe nanoparticles on bacterial growth and biosurfactant production. J. Nanopart. Res. 2013;15(1):1-13.
8. Kiran GS, Nishanth LA, Priyadharshini S, Anitha K, Selvin J. Effect of Fe nanoparticle on growth and glycolipid biosurfactant production under solid state culture by marine Nocardiopsis sp. MSA13A. BMC Biotech. 2014;14(1):48.
9. Nezahat B, Nebahat D, Dilhan M. Conversion of biomass to fuel: transesterification of vegetable oil to biodiesel using KF loaded nano-g-Al 2 O 3 as catalyst. Appl Catal B. 2009;89:590-6.
10. El-Sheshtawy H, Khalil N, Ahmed W, Abdallah R. Monitoring of oil pollution at Gemsa Bay and bioremediation capacity of bacterial isolates with biosurfactants and nanoparticles. Mar. Pollut. Bull. 2014;87(1):191-200.
11. Wehrli B, Sulzberger B, Stumm W. Redox processes catalyzed by hydrous oxide surfaces. Chem. Geol. 1989;78(3):167-79.
12. Auffan M, Achouak W, Rose J, Roncato M-A, Chanéac C, Waite DT, et al. Relation between the redox state of iron-based nanoparticles and their cytotoxicity toward Escherichia coli. Environ. Sci. Technol. 2008;42(17):6730-5.
13. Kiran GS, Thomas TA, Selvin J. Production of a new glycolipid biosurfactant from marine Nocardiopsis lucentensis MSA04 in solid-state cultivation. Colloids Surf., B. 2010;78(1):8-16.
14. Haferburg G, Kothe E. Microbes and metals: interactions in the environment. J. Basic Microbiol. 2007;47(6):453-67.
15. Jo W, Freedman KJ, Kim MJ. Metallization of biologically inspired silica nanotubes. Mater. Sci. Eng., C. 2012;32(8):2426-30.
16. Hendraningrat L, Li S, Torsæter O. A coreflood investigation of nanofluid enhanced oil recovery. J. Pet. Sci. Eng. 2013;111:128-38.
17. Marchant R, Banat IM. Biosurfactants: a sustainable replacement for chemical surfactants? Biotechnol. Lett. 2012;34(9):1597-605.
18. Yela ACA, Martínez MAT, Piñeros GAR, López VC, Villamizar SH, Vélez VLN, et al. A comparison between conventional Pseudomonas aeruginosa rhamnolipids and Escherichia coli transmembrane proteins for oil recovery enhancing. Int. Biodeterior. Biodegrad. 2016;112:59-65.
19. Tahseen R, Afzal M, Iqbal S, Shabir G, Khan QM, Khalid ZM, et al. Rhamnolipids and nutrients boost remediation

of crude oil-contaminated soil by enhancing bacterial colonization and metabolic activities. Int. Biodeterior. Biodegrad. 2016;115:192-8.
20. Hassan M, Essam T, Yassin AS, Salama A. Optimization of rhamnolipid production by biodegrading bacterial isolates using Plackett–Burman design. Int. J. Biol. Macromol. 2016;82:573-9.
21. Liu Y, Majetich SA, Tilton RD, Sholl DS, Lowry GV. TCE dechlorination rates, pathways, and efficiency of nanoscale iron particles with different properties. Environ. Sci. Technol. 2005;39(5):1338-45.
22. Wang J, Liu Q. Structural change and characterization in nitrogen-incorporated SBA15 oxynitride mesoporous materials via different thermal history. Microporous and mesoporous materials. 2005;83(1):225-32.
23. Saad R, Thiboutot S, Ampleman G, Dashan W, Hawari J. Degradation of trinitroglycerin (TNG) using zero-valent iron nanoparticles/nanosilica SBA-15 composite (ZVINs/SBA-15). Chemosphere. 2010;81(7):853-8.
24. Sharma A, Soni J, Kaur G, Kaur J. A Study on biosurfactant production in Lactobacillus and Bacillus sp. Int J Curr Microbiol App Sci. 2014;3(11):723-33.
25. Cooper DG, Goldenberg BG. Surface-active agents from two Bacillus species. Appl. Environ. Microbiol. 1987;53(2):224-9.
26. Diniz Rufino R, Moura de Luna J, de Campos Takaki GM, Asfora Sarubbo L. Characterization and properties of the biosurfactant produced by Candida lipolytica UCP 0988. Electron. J. Biotechnol. 2014;17(1):6-.
27. Mostafa NY, Al-Wakeel SAS, El-Korashy SA, Brown PW. Characterization and evaluation of the pozzolanic activity of Egyptian industrial by-products: I: Silica fume and dealuminated kaolin. Cem. Concr. Res. 2001;31(3):467-74.
28. Zhang JL SR, Misra RDK. Core-Shell Magnetite Nanoparticles Surface Encapsulated with Smart Stimuli-Responsive Polymer: Synthesis, Characterization, and LCST of Viable Drug-Targeting Delivery System. Langmuir. 2007;23:6342-51.
29. Al-Bahry S, Al-Wahaibi Y, Elshafie A, Al-Bemani A, Joshi S, Al-Makhmari H, et al. Biosurfactant production by Bacillus subtilis B20 using date molasses and its possible application in enhanced oil recovery. Int. Biodeterior. Biodegrad. 2013;81:141-6.
30. Dubey K, Juwarkar A. Distillery and curd whey wastes as viable alternative sources for biosurfactant production. World J. Microbiol. Biotechnol. 2001;17(1):61-9.
31. Kiran GS, Hema T, Gandhimathi R, Selvin J, Thomas TA, Ravji TR, et al. Optimization and production of a biosurfactant from the sponge-associated marine fungus Aspergillus ustus MSF3. World J. Microbiol. Biotechnol. 2009;73(2):250-6.
32. Lawrance A, Balakrishnan M, Joseph TC, Sukumaran DP, Valsalan VN, Gopal D, et al. Functional and molecular characterization of a lipopeptide surfactant from the marine sponge-associated eubacteria Bacillus licheniformis NIOT-AMKV06 of Andaman and Nicobar Islands, India. Mar. Pollut. Bull. 2014;82(1):76-85.
33. Reis RS, Da Rocha SLG, Chapeaurouge DA, Domont GB, Santa Anna LMM, Freire DMG, et al. Effects of carbon and nitrogen sources on the proteome of Pseudomonas aeruginosa PA1 during rhamnolipid production. Process Biochem. 2010;45(9):1504-10.
34. Huang X, Shen C, Liu J, Lu L. Improved volatile fatty acid production during waste activated sludge anaerobic fermentation by different bio-surfactants. Chem. Eng. J. 2015;264:280-90.
35. Shan G, Xing J, Zhang H, Liu H. Biodesulfurization of dibenzothiophene by microbial cells coated with magnetite nanoparticles. Appl. Environ. Microbiol. 2005;71(8):4497-502.
36. Ehrlich H. Microbes and metals. Appl. Microbiol. Biotechnol. 1997;48(6):687-92.
37. Liu J, Vipulanandan C. Effects of Au/Fe and Fe nanoparticles on Serratia bacterial growth and production of biosurfactant. Mater. Sci. Eng., C. 2013;33(7):3909-15.
38. Devi LS, Joshi SR. Evaluation of the antimicrobial potency of silver nanoparticles biosynthesized by using an endophytic fungus, Cryptosporiopsis ericae PS4. J. Microbiol. 2014;52(8):667-74.
39. Zhang L, Jiang Y, Ding Y, Daskalakis N, Jeuken L, Povey M, et al. Mechanistic investigation into antibacterial behaviour of suspensions of ZnO nanoparticles against E. coli. J. Nanopart. Res. 2010;12(5):1625-36.
40. Cabiscol E, Tamarit J, Ros J. Oxidative stress in bacteria and protein damage by reactive oxygen species. Int. Microbiol. 2010;3(1):3-8.
41. Choi O, Yu C-P, Fernández GE, Hu Z. Interactions of nanosilver with Escherichia coli cells in planktonic and biofilm cultures. Water Res. 2010;44(20):6095-103.
42. Cecchin I, Reddy KR, Thomé A, Tessaro EF, Schnaid F. Nanobioremediation: Integration of nanoparticles and bioremediation for sustainable remediation of chlorinated organic contaminants in soils. Int. Biodeterior. Biodegrad. 2016.
43. Chaithawiwat K, Vangnai A, McEvoy JM, Pruess B, Krajangpan S, Khan E. Impact of nanoscale zero valent iron on bacteria is growth phase dependent. Chemosphere. 2016;144:352-9.
44. Tang YJ, Ashcroft JM, Chen D, Min G, Kim C-H, Murkhejee B, et al. Charge-associated effects of fullerene derivatives on microbial structural integrity and central metabolism. Nano Lett. 2007;7(3):754-60.
45. Espinosa-Cristóbal L, Martínez-Castañón G, Martínez-Martínez R, Loyola-Rodríguez J, Patiño-Marín N, Reyes-Macías J, et al. Antimicrobial sensibility of Streptococcus mutans serotypes to silver nanoparticles. Mater. Sci. Eng., C. 2012;32(4):896-901.
46. Dehner C, Morales-Soto N, Behera RK, Shrout J, Theil EC, Maurice PA, et al. Ferritin and ferrihydrite nanoparticles as iron sources for Pseudomonas aeruginosa. JBIC Journal of Biological Inorganic Chemistry. 2013;18(3):371-81.
47. Sansinenea E, Ortiz A. Secondary metabolites of soil Bacillus spp. Biotechnol. Lett. 2011;33(8):1523-38.
48. Ismail W, Al-Rowaihi IS, Al-Humam AA, Hamza RY, El Nayal AM, Bououdina M. Characterization of a lipopeptide biosurfactant produced by a crude-oil-emulsifying Bacillus sp. I-15. Int. Biodeterior. Biodegrad. 2013;84:168-78.
49. Bordoloi N, Konwar B. Microbial surfactant-enhanced mineral oil recovery under laboratory conditions. C Colloids Surf., B. 2008;63(1):73-82.
50. Liu Q, Lin J, Wang W, Huang H, Li S. Production of surfactin isoforms by Bacillus subtilis BS-37 and its applicability to enhanced oil recovery under laboratory conditions. Biochem. Eng. J. 2015;93:31-7.
51. Ayed HB, Jemil N, Maalej H, Bayoudh A, Hmidet N, Nasri M. Enhancement of solubilization and biodegradation of diesel oil by biosurfactant from Bacillus amyloliquefaciens AN6. Int. Biodeterior. Biodegrad. 2015;99:8-14.